Modal Space Sliding Mode Control of Structures

RAJESH ADHIKARI*

Department of Applied Mechanics and Engineering Sciences
University of California San Diego, La Jolla, CA 92093-0411, USA.

HIROKI YAMAGUCHI and TOSHIKI YAMAZAKI

Department of Civil and Environmental Engineering
Saitama University, 255 Shimo-Okubo, Urawa, Saitama 338, Japan.

*Formerly with Dept. of Civil and Envi. Engg, Saitama University, Japan.

SUMMARY

For dynamical systems expressed in state space form or for systems with nonclassical damping, the reduction of the structural model into the modal coordinates involves complex modal analysis with complex modal coordinates. Sliding mode control (SMC) is formulated herein in terms of such complex modal coordinates and the resulting control scheme is applied to the Benchmark problem[1] consisting of the building–AMD system. Model reduction is achieved on the basis of the spectral analysis as well as wavelet analysis of the response of the system. Suitable provision is then provided to eliminate the effects of the neglected higher modes on the control performance. It is seen that the performances of MS–SMC are comparable to those of LQG.

Keywords :   sliding mode control, benchmark problem, wavelet analysis,
              complex–eigenvalue analysis, complex modal analysis

INTRODUCTION

The active structural control has emerged as a potential technology for enhancing structural functionality and structural safety of civil engineering structures against natural loadings such as earthquake loadings and wind loadings. Over the past few decades, various control algorithms and control devices have been developed, modified and investigated by various groups of researchers working in different parts of the world. A need was thus felt to establish a benchmark problem so that researchers working around the globe could test the algorithms developed by themselves applied to a well defined problem and could compare with the other methods/algorithms developed by various researchers also working in the field of active structural control. As a result, an experimentally evaluated mathematical model (evaluation model) of a scaled building was set as the benchmark problem which is described in details in Spencer et al. (1997).[1]

Out of various control schemes studied by various researchers, sliding mode control (SMC) has also shown its potential of becoming a serious candidate as the control algorithm applied to the civil engineering structures.[2-6] The robustness against parameter variations as well as excitation uncertainties that is imparted to the SMC due to its nonlinear control action,[4 -12] could make SMC an attractive control algorithm when dealing with civil engineering structures where the external excitation constitutes the main uncertainty in the system.

Since only few lower modes of the most of the civil engineering structures are generally excited during wind or earthquake loadings, it is desirable to control only those critical or the dominant modes. Though the application of modal space reduction techniques and the control of the critical modes of vibration of civil engineering structures have been discussed in many published works,[13-15] SMC, in the past, has mainly been designed based on the equations of motion available in the physical

1

coordinates. In such cases, SMC can be designed based on both the sliding surface and nonlinear control action being defined in terms of the physical states of the system,[2-6] or in terms of the modal coordinates which are obtained from the modal analysis of the equations of motion assuming that the system damping is negligible. In such cases the modal coordinates are real and the design of SMC doesnot require special considerations. However, when the available structural model is in the state space consisting of state vectors, such as the evaluation model of the benchmark problem, or if the structure possesses nonclassical damping, the reduction of the state equations into the modal coordinates involves complex eigenvalue analysis involving complex modal vectors and complex modal coordinates. The design of SMC in such case is not straight forward.

In the present paper, we first identify the dominant vibration modes of the building–AMD system presented in the benchmark problem. The power spectrum based on the Fourier transform and the wavelet analysis[16,17] of the input and output of the structural response are used to identify the dominant modes of the structural vibration. A methodology is then presented to design SMC in terms of the complex modal coordinates. The control scheme described herein is termed as "modal space sliding mode control (MS–SMC)" to distinguish it from the conventional sliding mode control. The MS–SMC is designed based on the reduced order model in the modal space comprising of the previously identified dominant modes of vibration only. Suitable robustness against spillover caused by the neglected higher modes is provided in the control scheme. Simulation results based on the MS–SMC comprising of only first mode are finally presented and compared with LQG based example control presented in Spencer et al. (1997)[1] which used a 10–dimensional reduced order model.

PROBLEM SETTING

The benchmark problem as defined in Spencer et al. (1997),[1] is based on an actively controlled, three–story, single–bay, scaled building model. A single active mass driver (AMD) located at the top floor of the building model is used for control. The structure is mounted on a shaking table through which earthquake motions are applied to the structure. The first three modes of the structural system are 5.81 Hz, 17.68 Hz and 28.53 Hz, with associated damping ratios given, respectively, by 0.33%, 0.23% and 0.30%.

The evaluation model of the building–AMD system of the benchmark problem[1] is represented by

$$\dot{x} = \mathbf{A}x + \mathbf{B}u + \mathbf{E}\ddot{x}_g, \tag{1a}$$

$$y = \mathbf{C}_y x + \mathbf{D}_y u + \mathbf{F}_y \ddot{x}_g + \mathbf{v}, \tag{1b}$$

2

$$z = \mathbf{C}_z\mathbf{x} + \mathbf{D}_z u + \mathbf{F}_z \ddot{x}_g, \tag{1c}$$

where $\mathbf{x}$ is the 28–dimensional state vector, $\ddot{x}_g$ is the scalar ground acceleration, u is the scalar control input in voltage, $\mathbf{y} = [x_m, \ddot{x}_{a1}, \ddot{x}_{a2}, \ddot{x}_{a3}, \ddot{x}_{am}]^T$ is the measurable response, $\mathbf{z} = [x_1, x_2, x_3, x_m, \dot{x}_1, \dot{x}_2, \dot{x}_3, \dot{x}_m, \ddot{x}_{a1}, \ddot{x}_{a2}, \ddot{x}_{a3}, \ddot{x}_{am}]^T$ is the vector of response that can be regulated. Here x_i represent the displacement of the ith floor relative to the ground, x_m is the displacement of the AMD relative to the third floor, $\ddot{x}_{ai}$ is the absolute acceleration of the ith floor, $\ddot{x}_{am}$ is the absolute acceleration of the AMD mass, and $\mathbf{v}$ is the vector of measurement noises.

The control objective is to design a feedback controller that minimizes ten performance indices given in Spencer et al. (1997).[1] Five of the performance indices correspond to minimizing rms values of the response and other five indices correspond to minimizing the maximum displacement, accelerations and control voltage. Apart from these performance indices, the controller must also satisfy the control implementation constraints.

MODELING OF THE SYSTEM FOR CONTROL

Characteristics of the System Responses

For studying the dynamic characteristics of the evaluation model given in the benchmark problem,[1] two given scaled earthquake motions of El Centro and Hachinohe earthquakes are used. The characteristics of the earthquake inputs as well as the dynamic characteristics of the response of the evaluation model are represented in Figs. 1, 2, 3 and 4. Figs. 1 and 2 show the power spectrum, time series and wavelet coefficients of the earthquake input, whereas Figs. 3 and 4 represent those of the top story acceleration subjected to the earthquake motions. It is seen in Figs. 1 and 2 that the energy contents of the earthquake motion in a frequency range of 2.083 Hz to 8.334 Hz covering the first natural frequency of the structure (5.81 Hz), is comparable to the energy contents of the earthquake motion in a frequency range of 8.334 Hz to 33.335 Hz covering both of the second and third modal frequencies of the structure (17.68 Hz and 28.53 Hz respectively). However, it is evident from Fig. 3 and 4 that eventhough the earthquake energy imparted to the structure in all of its three structural modes are comparable, only the response of the first mode is significant and the contribution of the second and third modes is practically negligible.

Therefore, it can be concluded here that the structure can be modelled as a SDOF system in modal coordinates to represent the dynamic responses of the evaluation model. However, the uncertainties caused by the neglected higher modes and the potential of spillover problems caused by the neglected modes must be taken care of in the design of the controller.
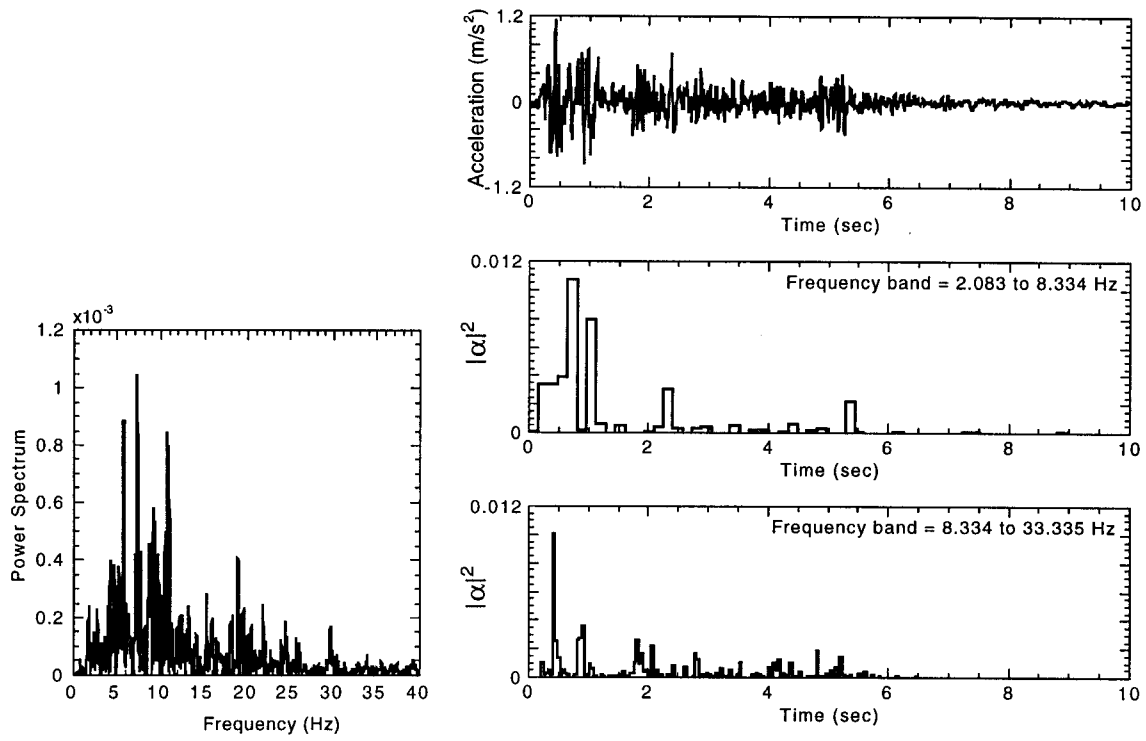
3

Fig. 1: Power spectrum, time series and wavelet coefficients of El Centro earthquake input.
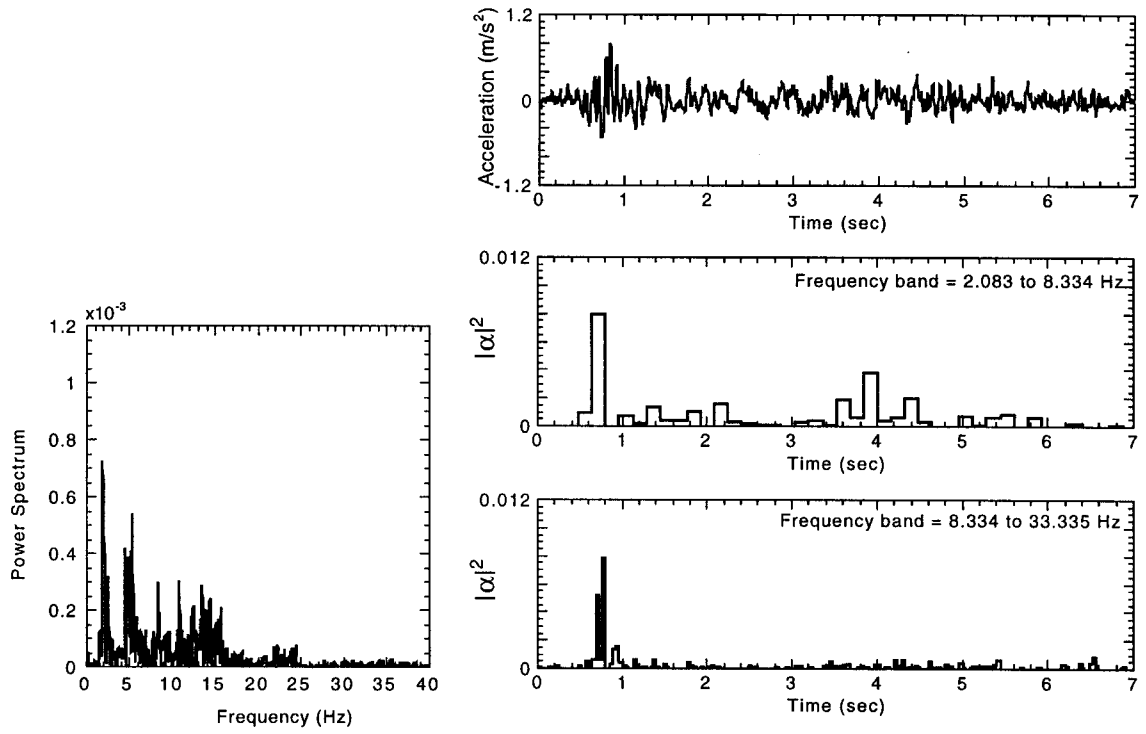

Fig. 2: Power spectrum, time series and wavelet coefficients of Hachinohe earthquake input.
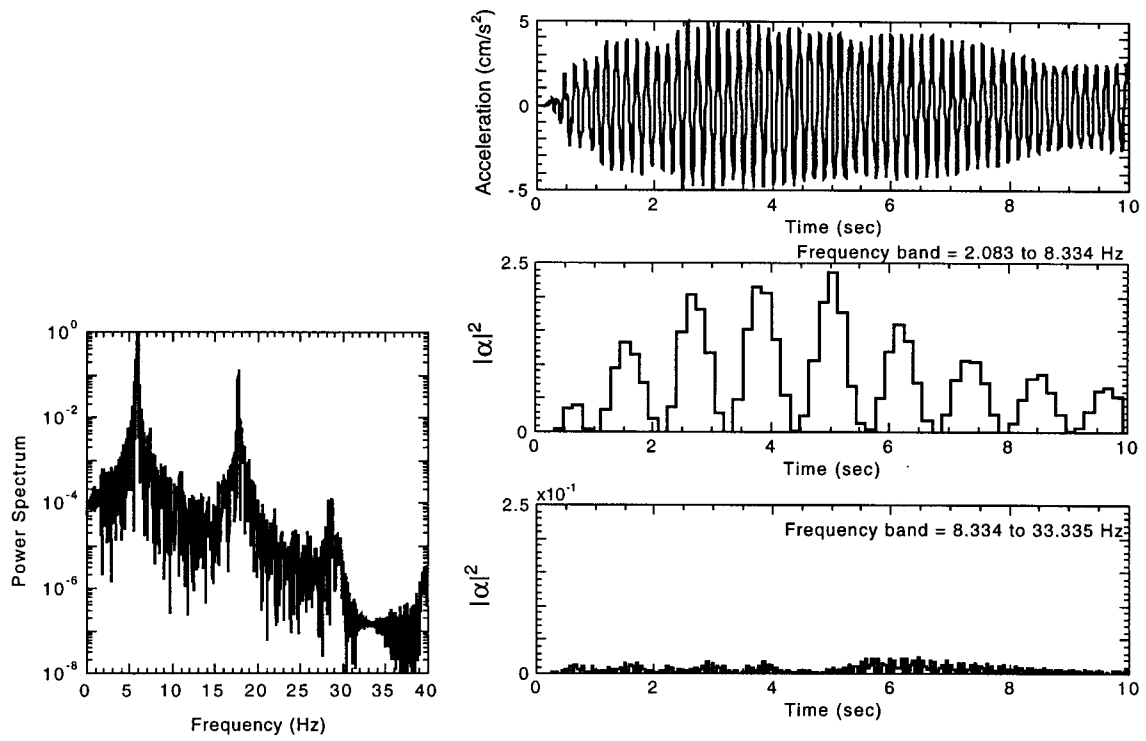
4

Fig. 3: Power spectrum, time series and wavelet coefficients of the top story acceleration subjected to El Centro earthquake.
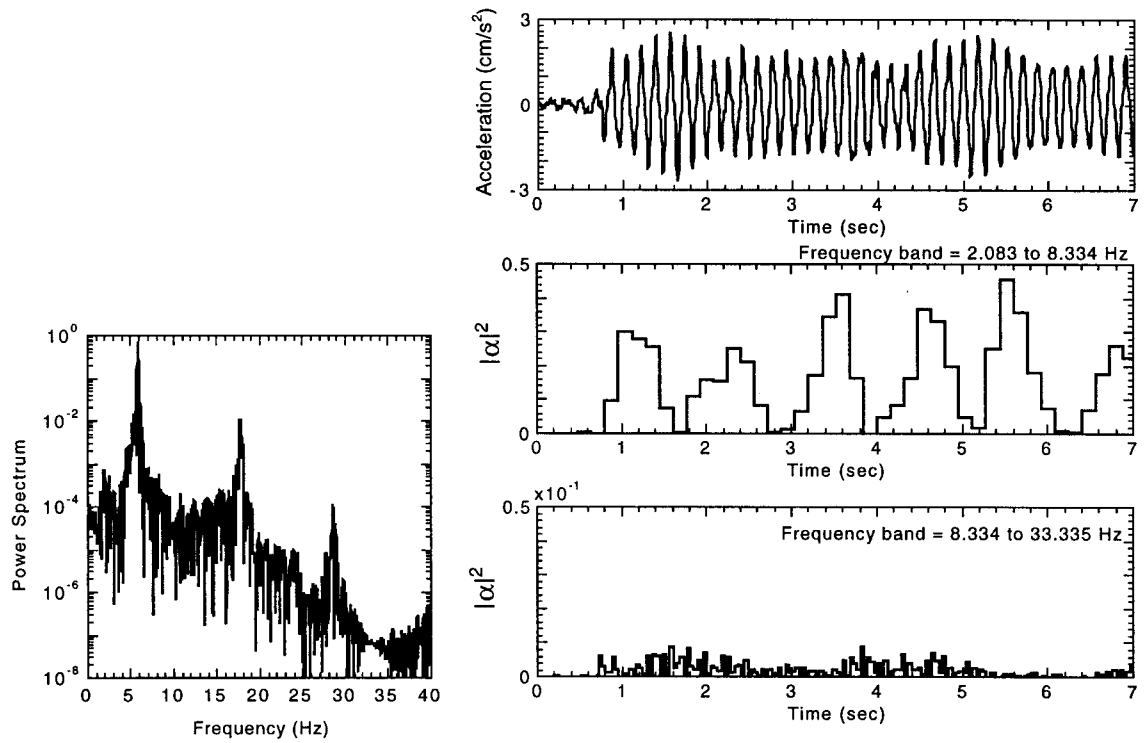

Fig. 4: Power spectrum, time series and wavelet coefficients of the top story acceleration subjected to Hachinohe earthquake.

Complex Modal Analysis

Neglecting the forcing terms of Eq. (1), we obtain the following equations for the modal analysis of the evaluation model

$$\dot{\mathbf{x}} = \mathbf{A}\mathbf{x}, \tag{2a}$$

$$\mathbf{z} = \mathbf{C}_z\mathbf{x}. \tag{2b}$$

The eigenvalue analysis of Eq. (2a) results in complex eigenvalues and complex eigenvectors related to the state vectors represented by $\mathbf{x}$.

It should be noted that because of the particular identification technique used in developing the evaluation model, the physical modes could be identified by using Eq. (2b) to obtain the physically meaningful modes ϕ_{zk} from ϕ_{xk} as

$$\phi_{zk} = \mathbf{C}_z\phi_{xk}. \tag{3}$$

The three structural modes were clearly identified by using Eq. (3) with ϕ_{xk} being the modal vectors obtained from the eigenvalue analysis of Eq. (2a). It should be noted that the structural modal vectors appear as complex conjugate pairs and that the corresponding modal coordinates appeared in the following modal analysis become complex conjugate pairs.

Following the usual method of modal analysis, the total response of the structure in the state space notations $\mathbf{x}$ can be represented as

$$\mathbf{x} = \mathbf{\Psi}_x\mathbf{p}, \tag{4}$$

where

$$\mathbf{\Psi}_x = [\mathbf{\Phi}_x \quad \mathbf{\Phi}_x^*], \tag{5a}$$

$$\mathbf{p} = [\mathbf{q}^T \quad \mathbf{q}^{*T}]^T. \tag{5b}$$

$\mathbf{p}$ in the above equations indicate the modal coordinates which also appear as complex conjugate pairs. For the ease in the mathematical treatment, the complex modal vectors and the complex modal coordinates in Eq. (5) are arranged such that complex and their conjugate parts appear separately.

Substituting Eq. (4) into the state equation Eq. (1a), multiplying the modal matrix $\mathbf{\Psi}_x$ to it and then making use of the following biorthonormal properties of the modal matrix[18]

$$\mathbf{\Psi}_x^T\mathbf{\Psi}_x = \mathbf{I} \quad \text{and} \quad \mathbf{\Psi}_x^T\mathbf{A}\mathbf{\Psi}_x = \mathbf{\Lambda}, \tag{6}$$

6

the equation of motion expressed in the state space become uncoupled and the modal equation of motions can be written as

$$\dot{\mathbf{q}} = \Lambda\mathbf{q} + \Psi_x^T \mathbf{B}u + \Psi_x^T \mathbf{E}\ddot{x}_g. \tag{7}$$

In the above equations, Λ is a diagonal matrix consisting of the complex eigenvalue λ_k of the matrix $\mathbf{A}$, and $\mathbf{I}$ is an identity matix.

Equation (7) represents the modal equations in complex modal coordinates and all of the terms appearing in Eq. (7) are complex quantities. It would be convinient to separate the modal equations into real and imaginary parts which would allow us to deal with real quantities and will thus simplify the formulation for control implementation. For this purpose, let the complex modal coordinate related to the k–th mode q_k, the corresponding complex modal vector ϕ_{xk} as well as the complex eigenvalue λ_k be represented as

$$q_k = \xi_k + i\eta_k, \qquad \phi_{xk} = \phi_{Rk} + i\phi_{Ik}, \qquad \lambda_k = \alpha_k + i\beta_k, \tag{8}$$

where subscript R stands for the real part while subscript I stands for the imaginary part of the complex quantities involved.

Substituting Eq. (5) into Eq. (7), utilizing Eq. (8), and then separating the real and imaginary parts, the following equations of motion for the k–th mode, are obtained in the real modal coordinates. [13,18]

$$\dot{\vartheta}_k = \mathbf{A}_k\vartheta_k + \mathbf{B}_k u + \mathbf{E}_k\ddot{x}_g, \tag{9}$$

where,

$$\vartheta_k = \begin{bmatrix} \xi_k & \eta_k \end{bmatrix}^T, \tag{10a}$$

$$\mathbf{A}_k = \begin{bmatrix} \alpha_k & -\beta_k \\ \beta_k & \alpha_k \end{bmatrix}, \tag{10b}$$

$$\mathbf{B}_k = \begin{bmatrix} \phi_{Rk}^T\mathbf{B} \\ \phi_{Ik}^T\mathbf{B} \end{bmatrix}, \tag{10c}$$

$$\mathbf{E}_k = \begin{bmatrix} \phi_{Rk}^T\mathbf{E} \\ \phi_{Ik}^T\mathbf{E} \end{bmatrix}. \tag{10d}$$

7

Reduced Order Model for Control

Considering only c modes for control, the structural model for control can be written as

$$\dot{\vartheta}_c = \mathbf{A}_c \vartheta_c + \mathbf{B}_c u + \mathbf{E}_c \ddot{x}_g. \tag{11}$$

The sensor output can be written as

$$\mathbf{y}_r = \mathbf{C}_{yr}^* \vartheta_c + \mathbf{C}_{yr}^{**} \vartheta_N + \mathbf{D}_{yr} u + \mathbf{F}_{yr} \ddot{x}_g + \mathbf{v}_r, \tag{12}$$

where $\mathbf{y}_r$ is obtained from $\mathbf{y} = [x_m, \ddot{x}_{a1}, \ddot{x}_{a2}, \ddot{x}_{a3}, \ddot{x}_{am}]^T$, depending on which output is used for feedback control and the corresponding $\mathbf{C}_{yr}^* = 2\mathbf{C}_{yr}[\mathbf{\Phi}_{Rc} \quad - \mathbf{\Phi}_{Ic}], \mathbf{C}_{yr}^{**} = 2\mathbf{C}_{yr}[\mathbf{\Phi}_{RN} \quad - \mathbf{\Phi}_{IN}]$, $\mathbf{C}_{yr}, \mathbf{D}_{yr}$ and $\mathbf{F}_{yr}$ are reduced order coefficient matrices obtained from the evaluation model defined in Eq. (1). Subscript N denotes the neglected modes. The matrices $\mathbf{A}_c, \mathbf{B}_c, \mathbf{E}_c$ as well as the modal state–vector ϑ_c of Eq. (11), can be easily obtained from Eq. (10) for the respective controlled modes.

When only c modes are considered, the structural response can be approximated by

$$\mathbf{x} = [\mathbf{\Phi}_c \quad \mathbf{\Phi}_c^*] \left\{ \begin{array}{c} \mathbf{q}_c \\ \mathbf{q}_c^* \end{array} \right\} = 2[\mathbf{\Phi}_{Rc} \quad - \mathbf{\Phi}_{Ic}] \left\{ \begin{array}{c} \xi_c \\ \eta_c \end{array} \right\}. \tag{13}$$

Once $\mathbf{x}$ is estimated, the physically meaningful response $\mathbf{z}$ is obtained by using Eq. (1c).

In the present paper, Eq. (11), alongwith the output relation given by Eq. (12), will be used to design the controller whereas the controller would be required to satisfy that the spillover problem and any potential instability caused by the neglected dynamics and observation errors due to the neglected dynamics given in Eq. (9b), are eliminated. The conceptual spillover mechanism is shown in Fig. 5 (also see, Juang et al. (1980)[14] and Balas (1980)[15]).

The benchmark problem states that the modal state vector ϑ_c is also to be estimated through the available observation vector $\mathbf{y}_r$. To this end, the Kalman filter optimal estimator similar to the one given in Spencer et al. (1997),[1] is used in the present study to evaluate the best estimate of the modal state vector. Let the best estimate of the modal state vector be represented by $\hat{\vartheta}_c$, then the Kalman filter optimal estimator is represented as

$$\dot{\hat{\vartheta}}_c = \mathbf{A}_c \hat{\vartheta}_c + \mathbf{B}_c u + \mathbf{L}(\mathbf{y}_r - \mathbf{C}_{yr}^* \hat{\vartheta}_c - \mathbf{D}_{yr} u). \tag{14}$$
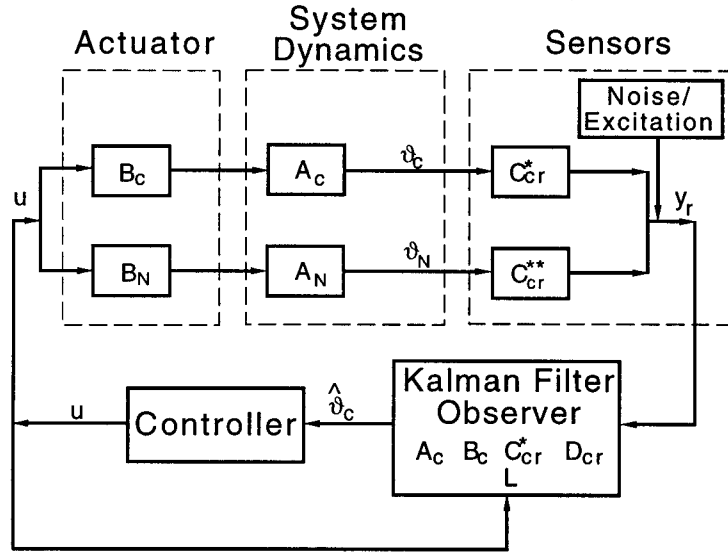
8

Fig. 5: Concept of spillover mechanism.

The Kalman filter gain **L** was determined by using the MATLAB routine lqew.m within the control toolbox. Similar to Spencer et al. (1997), here also the measurement noise is assumed to be identically distributed, statistically independent Gaussian noise processes, and $S_{\ddot{x}_g \ddot{x}_g}/S_{v_i v_i} = \gamma = 25$.

MODAL SPACE SLIDING MODE CONTROL (MS–SMC)

The nonlinear control force in the SMC framework for the present problem expressed in the modal coordinates, can be represented as,[11,12]

$$u(\hat{\vartheta}_c, t) = u_{\text{eq}}(\hat{\vartheta}_c, t) - \rho \text{sgn}(\sigma(\hat{\vartheta}_c)), \tag{15}$$

where u_{eq} is the linear part of the control force, known as the *equivalent control force*, ρ is a parameter which imparts discontinuity to the control action across the so called *sliding surface* $\sigma(\hat{\vartheta}_c)$ and sgn is the usual *signum* function, defined as $\text{sgn}(\sigma(\hat{\vartheta}_c)) = \sigma(\hat{\vartheta}_c)/|\sigma(\hat{\vartheta}_c)|$. If an observer has been properly designed so that it converges despite modeling uncertainties, then $\sigma(\hat{\vartheta}_c) \to \sigma(\vartheta_c)$. The magnitude of ρ, and thus the nonlinear control action, depends on the expected uncertainty in the external excitation or parameter variation.[8,12] It should be noted here that the control force as well as the sliding surface in the present case of MS–SMC depends on the modal quantities directly and hence provides a better means of modal control. In this case, it is no longer necessary to define the sliding surface based on the physical coordinates. The MS–SMC thus gives the flexibility of selecting only the particular modes that are to be controlled. However, the modal state vectors $\hat{\vartheta}$ are in fact related to the physical coordinates through Eq. (13) and Eq. (1c).

9

The equivalent control force u_{eq} of Eq. (15) is obtained by following the Utkin–Draženovic "method of equivalent control",[7,20] which states that in the sliding mode the system satisfies $\sigma(\hat{\boldsymbol{\vartheta}}_c) = 0$ and $\dot{\sigma}(\hat{\boldsymbol{\vartheta}}_c) = 0$, and the control force is the so called equivalent control force. For $\sigma(\hat{\boldsymbol{\vartheta}}_c) = \mathbf{S}\hat{\boldsymbol{\vartheta}}_c$, chosen to be a linear function of the states of the system, satisfying $\dot{\sigma}(\hat{\boldsymbol{\vartheta}}_c) = \mathbf{S}\dot{\hat{\boldsymbol{\vartheta}}}_c = 0$, yields

$$u_{eq}(\hat{\boldsymbol{\vartheta}}_c, t) = -(\mathbf{SB}_c)^{-1}\left[\mathbf{SA}_c\hat{\boldsymbol{\vartheta}}_c + \mathbf{SL}(\mathbf{C}_{yr}^{**}\boldsymbol{\vartheta}_N + \mathbf{F}_{yr}\ddot{x}_g)\right],\tag{16}$$

where $|(\mathbf{SB}_c)^{-1}| \neq 0$, and the sliding surface coefficient matrix $\mathbf{S}$ is a design matrix, usually constant, of size $r \times 2n$. Herein, r is the number of control inputs, which in the present case is equal to 1. The method of designing an optimal sliding surface coefficient matrix $\mathbf{S}$ is discussed in Utkin and Young.[21]

Clearly, the control law of Eq. (16) cannot be synthesized explicitly if the external excitation term $\ddot{x}_g$ is not known *a priori*, which is generally the case with the loading encountered with in the vibration problems related to civil engineering structures. However, under appropriate conditions, the control given in Eq. (16) can be synthesized implicitly via discontinuous (chattering) control defined in terms of the known system parameters. We, therefore, drop the term containing $\ddot{x}_g$ from Eq. (16) and, instead, through a properly selected value of ρ, impart a nonlinear switching discontinuous control action to account for the uncertainty in the excitation. If ρ is selected such that it accounts for the uncertainties caused by the neglected modes also, the term related to the neglected modes can also be dropped from Eq. (16). The choice of ρ and hence the control force $u(\hat{\boldsymbol{\vartheta}}_c, t)$ must be such that the existence and the attractiveness of the sliding mode is guaranteed.

In order to ensure the existence of a sliding surface and attractiveness to the surface, thereby guaranteeing stability of the system on the sliding surface, it is sufficient to choose a variable structure controller so that the following condition is satisfied[7,9,11]

$$\sigma(\hat{\boldsymbol{\vartheta}}_c)\dot{\sigma}(\hat{\boldsymbol{\vartheta}}_c) < 0.\tag{17}$$

For $\sigma(\hat{\boldsymbol{\vartheta}}_c) = \mathbf{S}\hat{\boldsymbol{\vartheta}}_c$, Eq. (17) together with Eq. (14), results in

$$\rho \geq |(\mathbf{SB}_c)^{-1}\mathbf{SL}(\mathbf{F}_{yr}\ddot{x}_g + \mathbf{C}_{yr}^{**}\boldsymbol{\vartheta}_N)|.\tag{18}$$

Therefore, the realizable control force is finally expressed as

$$u(\hat{\boldsymbol{\vartheta}}_c, t) = -(\mathbf{SB}_c)^{-1}\left[\mathbf{SA}_c\hat{\boldsymbol{\vartheta}}_c\right] - \rho\,\mathrm{sgn}(\sigma(\hat{\boldsymbol{\vartheta}}_c)),\tag{19}$$

where ρ is obtained from Eq. (18). Note that $\ddot{x}_g$ and $\boldsymbol{\vartheta}_N$ of Eq. (16) have been neglected in Eq. (19).

Please note that ρ as defined in Eq. (18), imparts nonlinear control action depending on the anticipated magnitude of excitation and the uncertainties caused by the neglected modes of vibration. Thus the problem of spillover due to the neglected modes can be reduced with a proper choice of ρ.

The direct implementation of the control given by Eq. (19), however, results in the so called *chattering* which is highly undesirable. Therefore, chattering is eliminated by smoothing the control force in a thin 'boundary layer' of thickness ϵ in the neighborhood of $\sigma(\hat{\vartheta}_c)$.[12] The control force without the chattering condition, is thus obtained as

$$u(\hat{\vartheta}_j, t) = -(\mathbf{SB}_c)^{-1}\mathbf{SA}_c\hat{\vartheta}_c - \rho\mathrm{sat}(\sigma(\hat{\vartheta}_c)/\epsilon), \tag{20}$$

where sat is a *saturation* function defined as

$$\mathrm{sat}(\sigma(\hat{\vartheta}_c)/\epsilon) = \begin{cases} \sigma(\hat{\vartheta}_c)/\epsilon, & \text{if } |\sigma(\hat{\vartheta}_c)/\epsilon| \leq 1, \\ \mathrm{sgn}(\sigma(\hat{\vartheta}_c)/\epsilon), & \text{otherwise.} \end{cases} \tag{21}$$

It should also be noted here that the control force as given by Eq. (20) results in a linear control inside the boundary layer for which the stability of the system is readily satisfied. However, as shown in Corless and Leitmann,[22] the control obtained here does not guarantee the asymptotic stability of the control system but the ultimate boundedness of trajectories within a neighbourhood of the origin, depending on ϵ, is guaranteed.

The performance of the control strategy developed herein is compared with the sample Linear Quadratic Gaussian (LQG) control design presented in Spencer et al. (1997).[1] The control design presented therein involves the following reduced order model.

$$\dot{\mathbf{x}}_r = \mathbf{A}_r\mathbf{x}_r + \mathbf{B}_r u + \mathbf{E}_r\ddot{x}_g \tag{22}$$

$$\mathbf{y}_r = \mathbf{C}_{yr}\mathbf{x}_r + \mathbf{D}_{yr}u + \mathbf{F}_{yr}\ddot{x}_g + \mathbf{v}_r \tag{23}$$

where $\mathbf{x}_r$ is a 10–dimensional state vector, $\mathbf{y}_r = \begin{bmatrix} \ddot{x}_{a1} & \ddot{x}_{a2} & \ddot{x}_{a3} & \ddot{x}_{am} \end{bmatrix}^T$ and $\mathbf{A}_r, \mathbf{B}_r, \mathbf{E}_r, \mathbf{C}_{yr}, \mathbf{D}_{yr}$ and $\mathbf{F}_{yr}$ are reduced order coefficient matrices as given in the reference.[1]

SIMULATION RESULTS AND DISCUSSIONS

Numerical simulations for each cases of excitations as given in Spencer et al. (1997)[1] were conducted using the MATLAB SIMULINK program. The evaluation model was

used to evaluate the control performance whereas the controller was designed based on the reduced order model. Only two measurement outputs $y_r = [\ddot{x}_{a3}, \ddot{x}_{am}]^T$, were used for the control. The sliding surface coefficient matrix S was obtained by following the method outlined in Utkin and Young (1978),[21] Nonami and Tian (1994),[23] and Yang et al. (1994).[3] This involved optimization of a performance index $J = \int_0^\infty \vartheta^T Q \vartheta dt$. Q for the present control design was selected to be $Q = \text{diag}[10, 1]$. The magnitude of the nonlinear control action σ was obtained from Eq. (18) by using the root mean square value of the ground acceleration (in volts) for each case of excitations. ρ thus obtained was assumed to be constant during the particular earthquake excitation for which it was obtained. The boundary layer thickness ϵ was assumed to be 0.1 for all of the simulations.

The performance of the MS–SMC controller of this study based on the 2–dimensional model, termed as 2D MS–SMC, is compared with the LQG controller given in Spencer et al. (1997)[1] which is based on a 10–dimensional reduced order model, hereafter referred to as 10D–LQG. The performance of both of the controllers for the case of El Centro excitation are shown in Fig. 6 for comparasion. Also shown in the same figure is the existance of the sliding mode in the modal space.

From Fig. 6, it can be concluded that the performance of the 2D MS–SMC is comparable or even better than that of the 10D–LQG as far as the reduction of the structural response is concerned. Also, there is no apparant spillover problem due to the neglected modes of the system. However, the increased controlled performance of the 2D MS–SMC comes at an expense of the increased controller activity. The maximum displacement as well as the maximum acceleration of the actuator can be considerable higher than those in case of the 10D–LQG. However, by making a proper choice of the sliding surface through various trials and errors, it may be possible to reduce the maximum response of the actuator. Reduction in the maximum response of the actuator, on the other hand, will increase the controlled response of the building thus resulting in the decrease in the control performance in terms of the reduction of the structural response.

The overall performances of the controller are tabulated in Table below. It is seen that, though the controller exhibit slightly increased activity, the performance of the 2D MS–SMC controller is comparable to those of 10D–LQG.

The RMS performance and constraint values were evaluated at the nominal design point ($\omega_g = 37.3 \frac{\text{rads}}{\text{sec}}$ and $\zeta_g = 0.3$) using a simulation duration of 300 seconds.
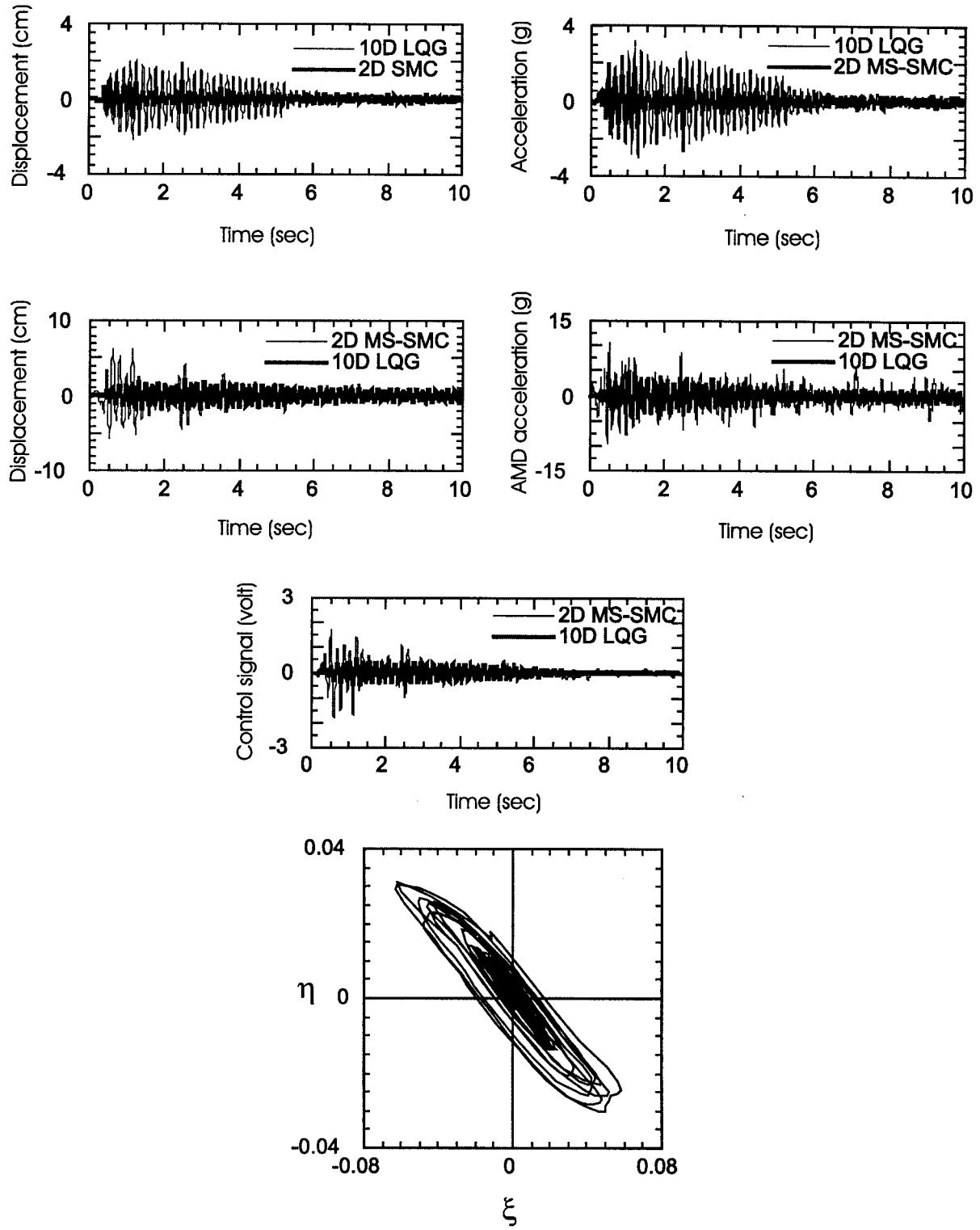
Fig. 6: The displacement and acceleration of the top floor, AMD (actuator) displacement and acceleration and control volt as obtained for MS–SMC and 10D–LQG, and the sliding mode in the modal space for MS–SMC.

Table. Performance of the 2D MS–SMC as compared to 10D–LQG.[1]

Performance Index	MS-SMC, designed for:			10D-LQG[1]
	Kanai-Tajimi	El Centro	Hachinohe	
J_1	0.1735	0.1728	0.1715	0.2840
J_2	0.2639	0.2625	0.2602	0.4397
J_3	1.2051	1.2188	1.2497	0.5114
J_4	1.0246	1.0328	1.0477	0.5125
J_5	1.1901	1.0744	1.0348	0.6267
J_6	0.3366	0.3354	0.3333	0.4556
J_7	0.5968	0.5917	0.5933	0.7102
J_8	3.3377	3.3333	3.3381	0.6680
J_9	3.4071	3.4467	3.5142	0.7753
J_{10}	2.8201	2.8734	3.0159	1.3360
σ_u (volts)	0.4210	0.4259	0.4372	0.1430
$\sigma_{\ddot{x}_{am}}$ (g)	2.1303	1.9233	1.8523	1.1218
σ_{x_m} (cm)	1.5787	1.5966	1.6371	0.6700
max $|u|$ (volts)	1.7903	1.8187	1.8611	0.5255
max $|\ddot{x}_{am}|$ (g)	10.8234	12.2059	12.3149	4.8275
max $|x_m|$ (cm)	6.3178	6.4301	6.5921	2.0017

CONCLUDING REMARKS

A modal space sliding mode control (MS–SMC) method is designed here which is applied to the Benchmark problem.[1] The power spectrum as well as the wavelet analysis of the time series of input output showed that the structure vibrated predominantly in the first natural frequency. Therefore, a single mode reduced order model of the system was first obtained for the design of the control, while suitable provision has been provided to eliminate the effects of the neglected higher modes. The performance of the MS–SMC based on single mode reduced order model is found to be quite satisfactory, though it involved higher controller activities. It is worth mentioning here that by making a proper choice of the sliding surface through various trials and errors, it may be possible to reduce the maximum response of the actuator. Reduction in the maximum response of the actuator, however, will increase the controlled response of the building thus resulting in the decrease in the control performance in terms of the reduction of the structural response.

REFERENCES

1. B. F. J. Spencer, S. J. Dyke, and H. S. Deoskar, 'Benchmark problems in structural control, Part I: Active Mass Driver System,' in *Proc. 1997 ASCE Structures Congress*, Portland, Oregon, April 13–16, 1997.

2. K. D. Young, 'Discountinuous control of sliding base isolated structures under earthquake,' in: *IMACS/SICE International Symposium on Robotics, Mechatronics and Manufacturing Systems*, Kobe, Japan, Sep. 16–20 1992.

3. J. N. Yang, J. C. Wu, A. K. Agrawal, and Z. Li, 'Sliding mode control for seismic-excited linear and nonlinear civil engineering structures,' *Technical Report, NCEER -94-0017*, 1994.

4. J. N. Yang, J. C. Wu, and A. K. Agrawal, 'Sliding mode control of seismically excited linear structures,' *ASCE, J. of Engineering Mechanics*, **121**(12), pp. 1330–1339, 1995.

5. J. N. Yang, J. C. Wu, and A. K. Agrawal, 'Sliding mode control of seismically excited nonlinear and hysteretic structures,' *ASCE, J. of Engineering Mechanics*, **121**(12), pp. 1386–1390, 1995.

6. J. N. Yang, J. C. Wu, A. M. Reinhorn, and M. Riley, 'Control of sliding–isolated buildings using sliding mode control,' *ASCE, J. of Structural Engineering*, **122**(2), pp. 83–91, 1996.

7. V. I. Utkin, 'Variable structure systems–present and future,' *Automation and Remote Control*, **44**(9), pp. 1105–1120, 1983.

8. E. P. Ryan, 'A variable structure approach to feedback regulation of uncertain dynamical systems,' *Int. J. Control*, **38**(6), pp. 1121–1134, 1983.

9. O. M. E. El-Ghezawi, A. S. Zinober, and S. A. Billings, 'Analysis and design of variable structure systems using a geometric approach,' *Int. J. Control*, **38**(3), pp. 657–671, 1983.

10. E. Bailey and A. Arapostathis, 'Simple sliding mode control scheme applied to robot manipulators,' *International J. of Control*, **45**(4), pp. 1197–1209, 1987.

11. R. A. DeCarlo, S. H. Zak, and G. P. Matthews, 'Variable structure control of nonlinear multivariable systems: A tutorial,' *Proceedings of the IEEE*, **76**(3), pp. 212–232, 1988.

12. J.-J. E. Slotine and W. Li, *Applied Nonlinear Control*, Prentice-Hall International Editions, 1991.

13. J. N. Yang and M. J. Lin, 'Optimal critical-mode control of building under seismic load,' *Journal of Engineering Mechanics Division, ASCE*, **108**(6), pp. 1157–1185, 1982.

14. J. N. Juang, S. Sae-Ung, and J. N. Yang, 'Active control of large building structures,' In *Structural Control*, North–Holland Publishing Co., Amsterdam, pp. 663–676, 1980.

15. M. Balas, 'Feedback control of flexible systems,' *IEEE Trans. on Automatic Control*, **AC–23**, pp. 673–679, 1978.

16. M. Yamada and K. Ohkitani, 'Orthonormal wavelet expansion and its application to turbulence. (Progress Letters),' *Progress of Theoretical Physics*, **83**(5), pp. 819–823, 1990.

17. M. Farge, 'Wavelet transform and their applications to turbulence,' *Annual Review of Fluid Mechanics*, **24**, pp. 395–457, 1992.

18. L. Meirovitch, *Dynamics and Control of Structures*, John Wiley & Sons, 1989.

19. MATLAB. The Math Works, Inc. Natic, Massachusetts, , 1994.

20. B. Draženovic, 'The invariance conditions in variable structure systems,' *Automatica*, **5**(3), pp. 287–295, 1969.

21. V. I. Utkin and K. D. Young, 'Methods for constructing discontinuous planes in multidimensional variable structure systems,' *Automation and Remote Control*, **31**, pp. 1466–1470, 1978.

22. M. J. Coreless and G. Leitmann, 'Continuous state feedback guaranteeing uniform ultimate boundedness for uncertain dynamic systems,' *IEEE Trans. on Automatic Control*, **AC–26**(5), pp. 1139–1144, 1981.

23. K. Nonami and H. Tian, *Sliding Mode Control (in Japanese)*, Corona Publishing Co. Ltd., Japan, 1994.